PROC. OF JSCE
No. 322, June 1982
[Technical Note]

FATIGUE CRACK GROWTH RATES IN STRUCTURAL STEELS

Toshie OKUMURA, Toshio NISHIMURA**, Chitoshi MIKI*** and Kinji HASEGAWA*****

1. INTRODUCTION

Application of the relationship $da/dN = C(\Delta K)^m$ (da/dN: fatigue crack growth rate, ΔK: stress intensity factor range, C, m: material constants)[1] is effective in the analysis of fatigue crack growth life. The values of material constants C and m have great influences on the predicted growth life. Barsom[2] calculated the values of C and m that determine the upper and lower bounds of the fatigue crack growth rates from experimental results.

Although the applicability of the Barsom's relationship has been studied for many steels produced in the U.S.A., no similar study has been performed on Japanese structural steels. The Study Group on Fatigue, a subcommittee of Steel Superstructures for Honshu-Shikoku Bridges of Japan Society of Civil Engineers, obtained data on the fatigue crack growth rate and attempted a similar analysis to that of Barsom's on Japanese steels. Since individual numerical data which are necessary for these analysis have not been supplied by the Japanese steel and bridge manufacturers, a similar analysis cannot be performed.

Without using individual numerical $da/dN-\Delta K$ data, we determined the representative da/dN and ΔK relationship through a C and m correlation[3),4),5)] obtained from the Paris law data supplied by Japanese steel and Bridge manufacturers. Furthermore, fatigue crack growth properties of various materials were studied through the analysis of the C and m correlation.

2. DESCRIPTION OF ORIGINAL DATA

The number of data (Paris Law relationships) submitted to the committee on the various types of steel and materials are summarized in **Table 1**. It is known that there are differences in fatigue crack growth characteristics between SM58 and HT80, which are quenched and tempered steels, and SM41 and SM50, which are not quenched and tempered steels. Therefore, a separate set of fine lines representing the Paris Law relationships for SM41 and SM50, and SM58 and HT80 are shown in **Fig. 1** and **Fig. 2** respectively.

Line 1 in **Fig. 1** correspond to the upper bound

Table 1 Number of data.

Steels \ Materials	Base metal	Weld metal	Heat affected zone	Remarks
SM41*	19	6	5	Carbon steel
SM50*	18	5	9	Low alloy steel
SM58*	22	9	8	Quenched and tempered high strength steel
HT80	27	8	4	

* : JIS G 3106
HT80 : 800 MPa class high tensile strength steel

* Member of JSCE, Dr. of Eng., Emeritus Professor, University of Tokyo
** Member of JSCE, Dr. of Eng., Professor, Dept. of Construction Engineering, Gunma University
*** Member of JSCE, Dr. of Eng., Associate Professor, Dept. of Civil Engineering, Tokyo Institute of Technology.
**** Graduate Student, Dept. of Civil Engineering, University of Tokyo

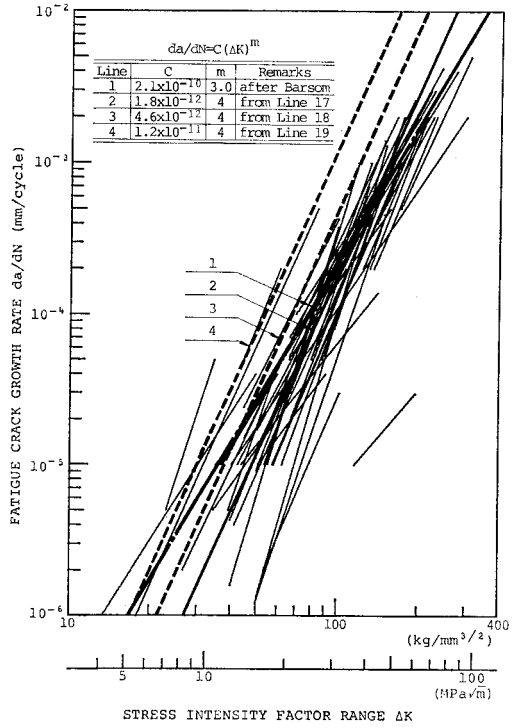

Fig. 1 Summary of da/dN-ΔK relationships of SM41, SM50.

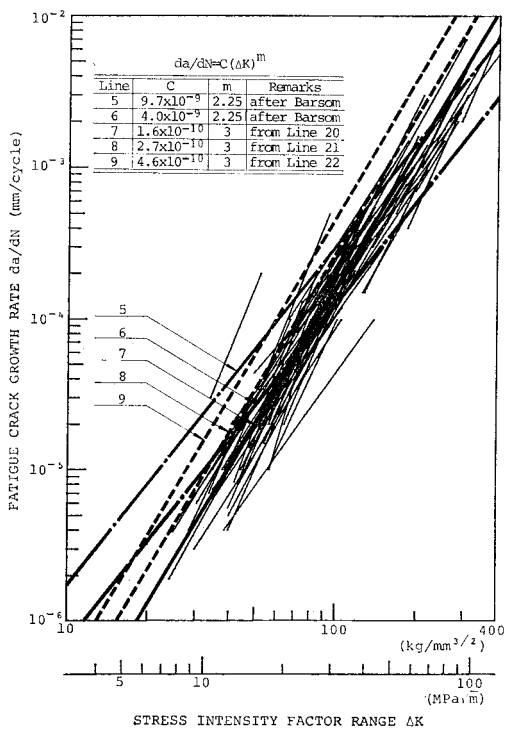

Fig. 2 Summary of da/dN-ΔK relationships of SM58, HT80.

of the fatigue crack growth rate for ferrite-pearlite steels; and, lines 5 and 6 in **Fig. 2** correspond to upper and lower bounds of the fatigue crack growth rate for martensite steels as calculated by Barsom[2]. As can be seen from these figures, many lines exists above and below these calculated bounds. In addition, the slope for lines 5 and 6 in **Fig. 2** is small in comparison with the individual slopes obtained from original data.

3. CORRELATION BETWEEN C and m

Since C and m are available from the original data, we plotted the coefficient on a semilogarithmic graph. Data points for various materials fall almost on a straight line indicated by equation (1). The correlation coefficient calculated from these data points is -0.981.

$$C=A/B^m \quad \cdots\cdots (1)$$

where A and B are constants.

Fig. 3 shows that scattering of C increases as m increases. Considering C as a random variable of m, constants A and B in equation (1) were calculated based on the hypotheses below:

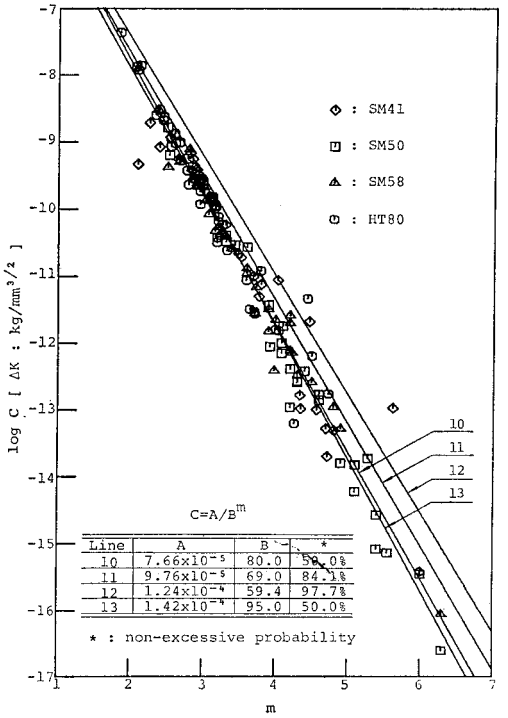

Fig. 3 Correlation between m and C of all steels.

Hypothesis 1: C follows a normal logarithmic distribution for a certain constant m.

Hypothesis 2: The average value (μ) and standard deviation (σ) of log C vary linearly with m.

Based on Hypothesis 1, the probability density function $P(C)$ is expressed by equation (2).

$$P(C)=\frac{1}{\sqrt{2\pi}\,\sigma C}\exp\left[-\frac{(\log C-\mu)^2}{2\sigma^2}\right] \quad \cdots\cdots(2)$$

Based on Hypothesis 2, μ and σ are expressed as follows:

$$\mu=a_1+a_2m \quad \cdots\cdots(3)$$

$$\sigma=a_3+a_4m \quad \cdots\cdots(4)$$

For the determination of the coefficient a_1, a_2, a_3 and a_4, the maximum likelihood estimation method is used. In effect, we selected the coefficient a_1-a_4, that makes the likelihood function L, equation (5) maximum.

$$L=\sum_{i=1}^{n}\frac{1}{\sqrt{2\pi}(a_3+a_4m_i)C_i}\exp\left[-\frac{(\log C_i-a_1-a_2m_i)^2}{2(a_3+a_4m_i)^2}\right] \quad \cdots\cdots(5)$$

When all of the data on C and m are substituted in the above equation, the following values are obtained:

$a_1=-4.12$ $\quad a_2=-1.90$

$a_3=0.105$ $\quad a_4=0.0645$

In **Fig. 3**, the values of A and B for the non-excessive probabilities at 50% (log $C=\mu$), 84.1% (log $C=\mu+\sigma$) and 97.7% (log $C=\mu+2\sigma$) are tabulated. The correlation line for 50% non-excessive probability (line 10) is similar to the results calculated by Koshiga[4] and Gurney[5]

In obtaining A and B for line 13 (**Fig. 3**) we made m the random variable of C. All other conditions are the same as for line 10. Since the absolute value of correlation coefficient is close to 1, it is natural that the difference between line 10 and 13 is small.

In **Fig. 4**, we compared the values of C and m for base metal (BM), weld metal (WM) and heat affected zone (HAZ) for SM58. Lines 14, 15 and 16 are the center lines calculated for each test material by the method of least squares. Although the number of data points for WM and HAZ are not as large as for BM, we can clearly observe that no difference exists in the values of C and m for the three different materials. Other steels also show the same trend.

Figs. 5 and **6** show the plots of C and m for SM41 and SM50, and SM58 and HT80, respectively. The values of A and B were calculated based on the hypotheses used for **Fig. 3**. By

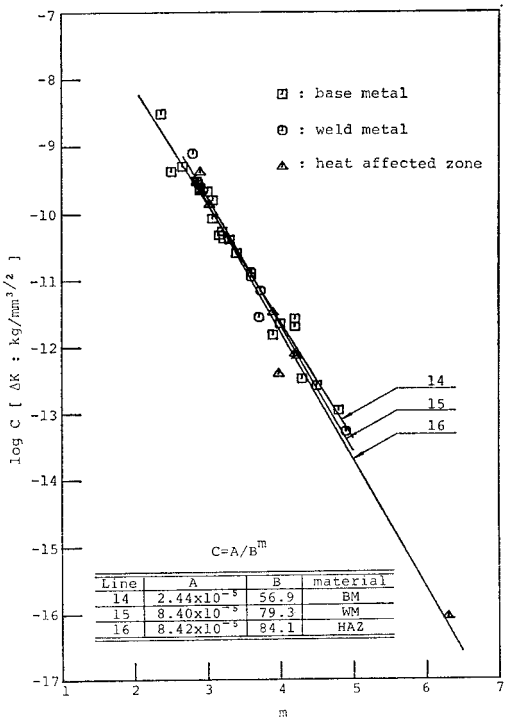

Fig. 4 Comparison of the relation between m and C for BM, WM and HAZ of SM58.

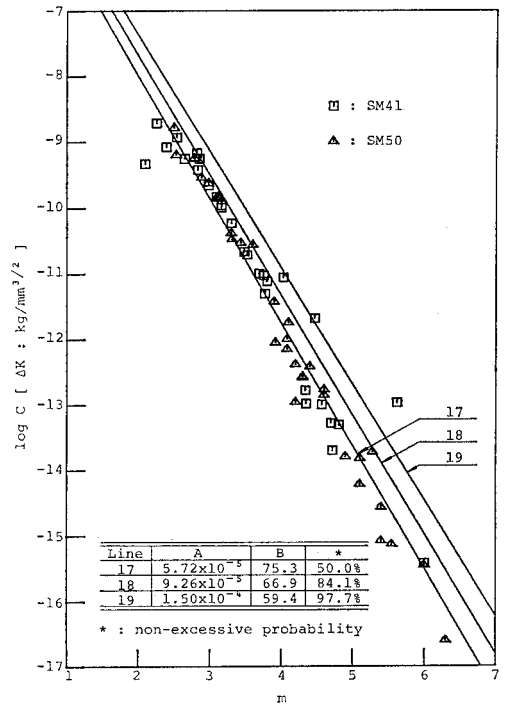

Fig. 5 Correlation between m and C of SM41 and SM50.

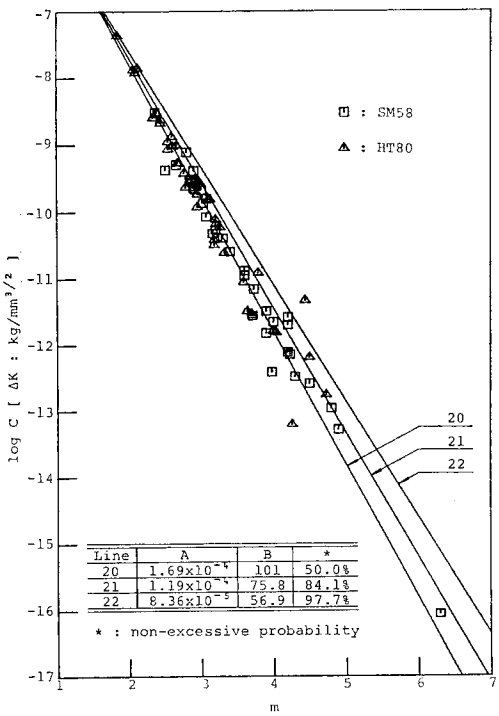

Fig. 6 Correlation between m and C of SM58 and HT80.

comparing the two figures, it is obvious that the data obtained from SM41 and SM50 have a wider range of C and m than the data obtained from SM58 and HT80.

The value of m is not constant for the wide range covered by the original data, hence we calculated m for four different regions of fatigue crack growth rate. We have provided average values of m for these regions. When one $da/dN-\Delta K$ line extends into more than one region, the same value of m is used for each region. Consequently, in the region of da/dN is 10^{-5}—10^{-3} mm/cycle (which is the linear Paris-Law region) the average value of m for SM41 and SM50 is 4, and for SM58 and HT80 is 3.

4. DETERMINATION OF REPRESENTATIVE da/dN-ΔK RELATIONSHIPS

The values of C corresponding to an m of 4 for SM41 and SM50, and 3 for SM58 and HT80, are obtained from the C-m relationships in **Figs. 5** and **6**. These $da/dN-\Delta K$ relationships are shown in **Figs. 1** and **2** (lines 2, 3 and 4 in **Fig. 1**, and 7, 8 and 9 in **Fig. 2**). The $da/dN-\Delta K$ relationship, using these C and m values which corresponds to a certain non-excessive probability of C, may not correspond to the original $da/dN-\Delta K$ relationships for the same non-excessive probability for the whole region of interests.

However, the $da/dN-\Delta K$ relationship obtained from the C-m correlationship for 50% non-excessive probability is located in the center of the original data lines. Also, the relationship obtained for 84.1% creates the upper bound for all of original data lines. Therefore, the two relationships (50% and 84.1%) for **Figs. 1** and **2** can be used as the representative $da/dN-\Delta K$ relationships for each material.

5. CONCLUDING REMARKS

Most of the original data used in this paper are above the fatigue crack growth rate of 10^{-5} mm/cycle. In actual structures, slow fatigue crack growth rate becomes the dominant factor in the determination of fatigue life. Therefore, we suggest more studies should be performed on the analysis of the slow growth fatigue crack characteristics.

6. ACKNOWLEDGEMENTS

The authors express their gratitude to Hitachi Shipbuilding, Ishikawajima-Harima Heavy Industries, Kawasaki Heavy Industries, Kawasaki Steel, Mitsui Engineering and Shipbuilding, Nippon Kokan, Sumitomo Metal Industries and Yokokawa Bridge Works for their permission to use their experimental data. The authors also wish to thank members of the Study Group on Fatigue for their valuable discussions and for letting us to publish this article.

REFERENCES

1) Paris, P. V. and F. Erdogan: A Critical Analysis of Crack Propagation Laws, Journal of Basic Engineering, Trans. of ASME, Vol. 85, pp. 528～535, 1963.
2) Rolfe, S. T. and J. M. Barsom: Fracture and Fatigue Controll in Structures, Prentices—Hall, Inc., pp. 236～239, 1977.
3) Kitagawa, H.: Fracture Mechanics Analysis of Fatigue Crack Growth (Part 1), Journal of the Society of Materials Science Japan, Vol. 26, No. 284, pp. 88～99, 1975-5 (in Japanese).
4) Koshiga, F. and M. Kawahara: A Proposed Design Basis with Special Reference to Fatigue Crack Propagation, Journal of the Society of Naval Architects in Japan, No. 133, pp. 305～312, 1973-6 (in Japanese).
5) Gurney, R. R.: Fatigue of Welded Structures, Second Edition, Cambridge University Press, pp. 53～64, 1979.

(*Received February 20, 1981*)